Wavebreaks and self-termination of spiral waves in a model of human atrial tissue

Irina V. Biktasheva[1], Vadim N. Biktashev[2], and Arun V. Holden[3]

[1] Department of Computer Science, Liverpool University, Liverpool L69 3BX, UK
ivb@csc.liv.ac.uk,
WWW home page: http://www.csc.liv.ac.uk/~ivb

[2] Department of Mathematical Sciences, Liverpool University, Liverpool L69 7ZL, UK

[3] School of Biomedical Sciences, Leeds University, Leeds LS2 9JT, UK

Abstract. We describe numerical simulations of spiral waves dynamics in the computational model of human atrial tissue with the Courtemanche-Ramirez-Nattel local kinetics. The spiral wave was initiated by cross-field stimulation protocol, with and without preliminary "fatigue" by rapid stimulation of the model tissue for a long time. In all cases the spiral wave has finite lifetime and self-terminates. However the mechanism of self-termination appears to depend on the initiation procedure. Spiral waves in the "fresh" tissue typically terminate after a few rotations via dissipation of the excitation front along the whole of its length. The dynamics of spiral waves in "tired" tissue is characterized by breakups and hypermeander, which also typically leads to self-termination but only after a much longer interval of time. Some features of the observed behaviour can not be explained using existing simplified theories of dynamic instabilities and alternanses.

1 Introduction.

In this paper we continue to investigate the behaviour of re-entrant waves of excitation in a computational model of human atrial tissue, which we started in [1]. The model showed spontaneous break-ups and self-termination of spiral waves, which can have relationship to mechanisms underlying atrial fibrillation, a condition that adversely affects quality of life and bears potential life threat. So despite all the limitations coming from simplified geometry, homogeneity and isotropy of our model, these results were suggestive and promising, and warranted further investigation. The mechanisms of breakups and self-termination of spirals in our computational model are far from understanding. In this paper we extend the study to different types of initial conditions and to different methods of analysis. The purpose of considering different initial conditions is to assess their effect on the re-entry behaviour. In the analysis of results of simulation, we assess, in particular, the feasibility of the "slope-one" theory, started by Nolasco and Dahlen [2] and given much prominence recently [3–6]; we refer to it as Nolasco-Dahlen (ND) theory for brevity. This theory has been tested and confirmed on some simplified models and some experimental preparations, although its universal applicability so far remains questionable [6]. In this paper we deliberately avoid discussing the basis of the theory, but restrict ourselves to purely phenomenological analysis of the results of simulations. Thus the structure of the paper is as of an experimental paper, with Section 2 dedicated to the methods, Section 3 to the results, and Section 4 to their discussion.

2 Methods: 2D model of human atrial tissue.

Excitation kinetics of cells. We used the human atrial action potential model by Courtemanche et al. [7] (CRN model) incorporated into a two-dimensional reaction-diffusion system of 21 partial differential equations.

Tissue model. We modelled the tissue as a continuous, homogeneous, isotropic, monodomain syncytium, i.e. in terms of "reaction+diffusion" system of equations, with diffusion term only in the equation for the transmembrane voltage,

$$\frac{\mathrm{d}\mathbf{u}}{\mathrm{d}t} = \mathbf{f}(\mathbf{u}) + \mathbf{D}\nabla^2\mathbf{u}$$

where $\mathbf{u} = (E, m, h, \dots)^T \in \mathbb{R}^{21}$ is the vector of the dynamic variables of the model, and $\mathbf{D} = \mathrm{diag}(D, 0, 0, \dots)$ is the matrix of diffusion coefficients, of which only the diffusion coefficient of the transmembrane voltage E is nonzero. This simplified description focuses on the excitation and propagation kinetics and allows interpretation in terms of numerous theories applicable to this kind of equations, while ignoring the additional complications due to geometry, anisotropy and heterogeneity of a real atrium. The diffusion coefficient of the transmembrane voltage $D = 0.03125\,\mathrm{mm}^2/\mathrm{ms}$ was set to give a plane wave velocity of $\approx 0.265\,\mathrm{mm/ms}$. Different D produce identical behaviour, only on a different spatial scale. The problem was posed in a square $75\,\mathrm{mm} \times 75\,\mathrm{mm}$ with no-flux boundary conditions for E.

The numerical scheme. The partial differential equations were solved using explicit Euler scheme in time, with time step $\Delta t = 0.1$ms, and simplest second-order approximation of the Laplacian space step $\Delta x = 0.2$mm.

Initial conditions Spiral waves in this study were initiated by the **cross-field stimulation method**. This is a widely used method for initiation of spiral waves, as it is relatively easy to implement both in the experiments and in the simulations.Our numerics used one or more of plane waves (*conditioning waves*) initiated to propagate from right to left of the medium; then at a certain moment, when the recovery tail of a wave is somewhere in the middle of the medium, we excited the lower half of the medium by instantly raising the transmembrane voltage by 100 mV in the lower part of the medium. This creates a new excitation front in the right half of the medium where it has recovered but not in the left which is still refractory. This broken excitation front quickly develops into a spiral wave. This is different from the **phase distribution method** whereby one-dimensional calculations are used to record values of all dynamical variables in a plane periodic wave of a high frequency, $\mathbf{U}(\phi)$, where $\mathbf{U} \in \mathbb{R}^{21}$ is the vector of dynamic variables of the model and $\phi \in \mathbb{R} \mod 2\pi$ is the phase within the period, and then the initial conditions are set as $\mathbf{u}(x, y, 0) = \mathbf{U}(\phi(x, t))$, where $\phi(x, y)$ is the distribution of the phase, chosen by will, e.g. corresponding to Archimedean spiral; thus the name of the method. The phase distribution method was used in our previous work [1] as it allowed quick generation of a spiral wave with the desired position of the core in the medium, and promised freedom from artificial inhomogeneities introduced by initial conditions. In present work, we used the cross-field stimulation as more realistic physiologically, and to see to what extent the behaviour of the spiral waves depends on the details of the initial conditions.

As in the case of phase-distribution method, the cross-field method can be implemented not only with 'fresh' medium but also with a 'tired' medium. The **fresh medium** was where the function $\mathbf{U}(\phi)$ and the conditioning waves are obtained by propagating a single wave through the medium, which prior to that was in the steady equilibrium 'resting state'. For the **tired medium**, this wave was the last wave in the series of a long (30 s long) series of rapid (period 300 ms) plane waves. There are 'superslow' variables in the model, which do not fully recover within a 300 ms excitation cycle; these changes accumulate over time which effectively amounts to change in the model parameters. Relevance of such changes in a particular model to any physiological condition is debatable, see [8] and references therein. Yet, these changes are relatively minor, and provide an example of physiologically feasible parameter variations, perhaps the best of what is achievable within the framework of this particular model and without involving further experimental data.

Thus, we had two sets of numerical experiments, with two different types of media, 'fresh' and 'tired'. This can be compared to two sets of simulations with similarly 'fresh' and 'tired' media but with phase-distribution initial conditions described in [1].

Processing of results. We depict the front propagation patterns as snapshots of the excitation field and by isochrone maps. **Snapshots** show distribution of the fields of $E(x, y, t)$, the transmembrane voltage, and $o_i(x, y, t)$, the inactivation gate of the transient outward current, as functions of x, y at fixed selected values of time t. On each snapshot, the red component of the colour of a point corresponds to the value of E, with zero corresponding to $E = -100\,\mathrm{mV}$ and maxium corresponding to $E = 50\,\mathrm{mV}$, and the green component of the colour corresponds to the value of o_i, with zero corresponding to $o_i = 0$ and the maximum corresponding to $o_i = 1$. By virtue of the excitation kinetics, the green and red colours are almost complement of each other. In black and white printed version, the regions with higher E (excited, systolic regions) are darker than the regions with higher o_i (unexcited, diastolic regions). **Isochrone maps** are collections of **isochrones**, i.e. instant positions of wavefronts or wavebacks, defined as fragments of isolines $E(x, y, t) = -40\,\mathrm{mV}$ which satisfy condition of

$o_i(x, y, t) > 0.5$ (wavefronts) or $o_i(x, y, t) < 0.5$ (wavebacks) for a given value of t. Correspondingly, the **wavebreak points**, and spiral **wave tips** are defined as internal ends of these fragments, i.e. intersections of isolines $E(x, y, t) = -40\,\mathrm{mV}$ and $o_i(x, y, t) = 0.5$. The moment of **self-termination** of the arrhythmia was defined as the moment of ultimate disappearance of all tips; this inevitably lead to eventual return of the medium to the uniform resting state when last excitation waves reach boundaries. **Restitution curves** are usually defined as dependence of the **action potential duration (APD)** of a cell on the preceding **diastolic interval (DI)** of that cell. In our numerics, we defined APD as a continuous interval of time t when $E(x, y, t) > E_*$ at a given point (x, y) and for a certain fixed E_*; correspondingly, DI is the interval when $E(x, y, t) < E_*$. We have tried different values of E_*.

3 Results

3.1 Fresh medium

We have made 7 simulations of spiral waves stimulated in the fresh medium, different in the initial position of the spiral wave with respect to the medium boundaries. This allowed us assess the effect of boundaries on the spiral wave dynamics. We describe in detail one simulation of this series. Figure 1 shows a collection of snapshots, from the moment of initiation by cross-field stimulation, $t = 0$, with an interval of $100\,\mathrm{ms}$ up to the frame $t = 1900\,\mathrm{ms}$, after which the spiral wave self-terminates, i.e. excitation fails to re-enter in the medium and eventually decays (not shown). As can be seen from the movie, but not necessary from the set of still pictures, the key event leading to the self-termination happens at around $t \approx 1400\,\mathrm{ms}$ and is characterized by block of propagation, at which the wavefront "dissipates" along a long line, stretching almost up to the upper boundary of the medium.

To visualize this and other important events, we employed the method of isochrone maps. The relationship between the snapshot and isochrone representation is illustrated by fig. 2, where a front isochrone, a tip and a back isocrhone are shown for a selected snapshot from the previous series.

The isochrone maps, i.e. collection of such isochrones for a selected intervals of times, separately for fronts and backs, are shown on fig. 3. Whereas propagation of fronts is more or less smooth everywhere where the fronts propagate at all, the evolution of the back is highly irregular, and this irregularity has a tendency to increase with time. This is a display of the "dynamic inhomogeneity" discussed in [1]. At times the irregularity reaches a stage where visual propagation of the back is opposite to the propagation of the previous front at that point. In extreme cases, one can see islands of recovered medium before the overall back of the wave reaches that site. One such episode can be seen on the panel of back isochrones for $t = 600 \ldots 900\,\mathrm{ms}$ in the left top quarter. This is the effect of "triggered recovery" [1, 9]. The inhomogeneity of the propagation pattern of wavebacks, with the relative homogeneity of the wavefronts, is an evidence of high variability of the action potential durations. This inhomogeneity affects propagation of

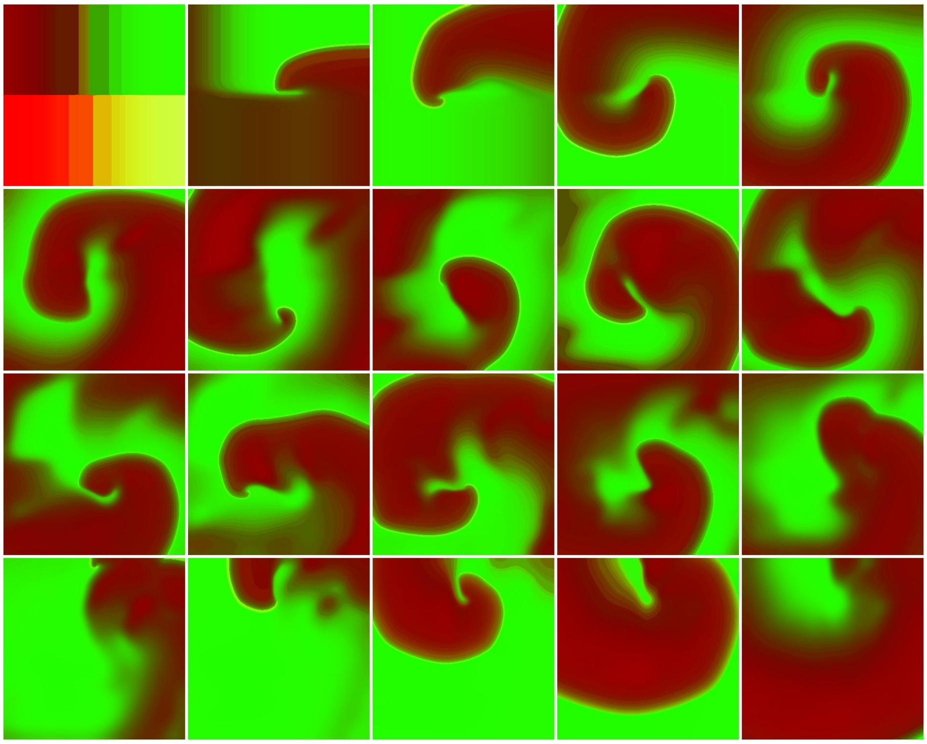

Fig. 1. (color online) Development of a spiral wave, initiated by cross-field stimulation in the fresh medium. Shown are snapshots with interval 100 ms, starting from 0 ms, in the "reading order" (left to right, then top to bottom).

next wavefronts either by slightly delaying or speeding them up, and from time to time by blocking next fronts, which leads to sudden displacement of the functional block of the spiral wave, which results in the highly irregular, "hyper-meander" trajectory of the spiral tip. This is likely to happen where the speed of recovery wave is slow, which shows as dense location of back isochrones. The above mentioned key event of front propagation block is clearly seen on front isochrone map $t = 1200 \ldots 1500$ ms as a long almost straight trajectory of the wavetip at which the wavefronts retract rather than protrude; this is a visual effect of wavefronts actually dissipating when reaching that line. This event is preceded by a density of wavebacks, which is seen on back isochrone maps of $t = 900 \ldots 1200$ ms (from approx. 1000 ms on) and $t = 1200 \ldots 1500$ ms (up until approx. 1300 ms), which occurs right at the site where subsequent fronts are blocked.

A distinct feature of the above discussed simulation is a relatively short lifetime of the spiral wave, 1776 ms. Other 6 simulations with different initial positions of the spiral showed similarly short lifetimes, from 1732 ms to 2732 ms, with average and standard deviation of 1900 ± 367 ms for all 7 simulations.

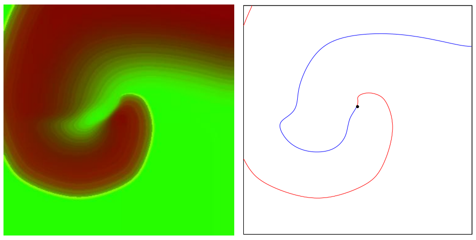

Fig. 2. (color online) Alternative representations of an excitation pattern. Left: snapshot $t = 300\,\mathrm{ms}$ from fig. 1. Right: the same, represented by isoline $E = -40\,\mathrm{mV}$, the 'isochrone'. The dot on the line is the tip of the spiral, defined by the additional condition $o_i = 0.5$. This point splits the isoline to two parts, front (red) and back (blue).

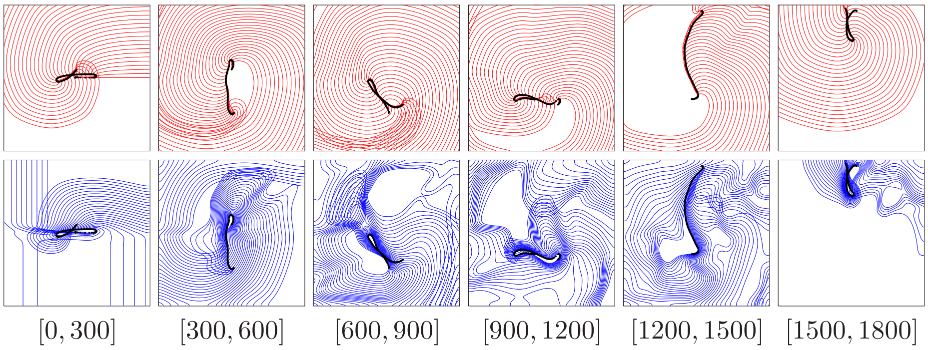

Fig. 3. (color online) Isochronal maps corresponding to fig. 1. Time interval between isochrones is 10 ms. Fronts are on upper panels, backs are on lower panels. Bold points, blending together into thick black lines, are the free ends of the isochrones, i.e. tips of the spirals.

3.2 Tired medium

Figures 4 and 5 show evolution of a spiral wave in a selected simulation with a tired medium. The lifetime of this spiral wave was 6992 ms, i.e. much longer than those in a fresh medium. Figure 4 shows snapshots in the first 3400 ms of that interval and fig. 5 shows isochrones in the first 1500 ms of it.

As in the fresh medium, there is prominent dynamic inhomogeneity caused by variability of APD and reflected by irregular patterns of the waveback isochrones. However, this time the irregularity seems less, although we didn't measure it by any formal measure. As a result, the dynamic imhomogeneity does not develop a complete block of the propagation and instead shows localized block of propagation, i.e. a breakup of the wave. The analysis of the record of the wavebreak points in the numerics of figs. 4,5 shows that the breakups lead to generation of new pairs of spiral waves which occur both nearly in the same place and each exist for about one period before annihilating, in the intervals $t = 770 \ldots 874\,\mathrm{ms}$ and

$t = 1132 \dots 1258\,\mathrm{ms}$ (although at different definition of wavebreaks this could perhaps be considered as one pair of spirals which existed for two rotations).

Evolution in other two simulations with the tired medium showed similar types of evolution and similarly large lifetimes of the spirals, from 4034 ms to 9924 ms with average and standard deviation of 3 simulations $6983 \pm 2945\,\mathrm{ms}$.

3.3 De-facto restitution properties

The ND theory and its variations aim to describe precisely the kind of process, when the action potential duration (APD) variability in response to the history of excitation causes instability of regular propagation of waves. This theory is based on the relationship between the diastolic interval (DI) and subsequent APD. To test how much this theory can be applied to our model, we have recorded values of transmembrane voltage, $E_j(t) = E(x_j, y_j, t)$, for a regular grid of 13×13 points (x_j, y_j), $j = 1 \dots 269$ regularly spread through the medium. We have tried different values of E_* for defining APD and DI. Figure 6 shows a typical electrogram in relation to voltages $E_* = -33\,\mathrm{mV}$, corresponding to $\bar{m}(E_*) = 1/2$, $E_* = -67\,\mathrm{mV}$, which corresponds to $\bar{h}(E_*) = 1/2$, and $E_* = -50\,\mathrm{mV}$ which is the average of the two, i.e. in the middle of the fast Na current excitation window. We see that the high variability of action potential profiles makes any of these voltages not ideal for determining APD and DI, although, arguably, $E_* = -67\,\mathrm{mV}$ looks more sensible than the other two.

The graphs of APD vs DI for the three selected values of E_* are shown on fig. 7. We believe that even bearing in mind all possible sources of errors, these graphs are an evidence that DI is not a good predictor of APD at all.

4 Discussion

We have found that the difference in the initial condition does not qualitatively change the behaviour of spiral waves in this model of atrial tissue. As in [1], we see that the evolution of spiral waves is dominated by such factors as developing dynamic inhomogeneity, including triggered recovery, which causes localized or massive dissipation events of wavefronts, which in turn lead to hypermeander of the tip of the spiral, spontaneous generation of new spirals, and eventually to self-termination of all re-entrant activity. The new study confirms that the time to self-termination in a tired medium is much longer than in the fresh medium.

This finding seems to suggest a possible mechanism of proarrhythmic action of tissue fatigue. However, it is not certain how our "numerical fatigue" relates to physiology. So the theoretical aspect, the mechanism of the development of the dynamic inhomogeneity, may be even more important. The ND theory explains the dynamic inhomogeneity based on the assumption that an APD is determined by the immediately preceding DI. This works for some models [5]. However, this assumption does not seem to bear any resemblance to the processes happening in this model. Perhaps, correct predictors of APD can be found based on asymptotic analysis of the realistic excitability models, rather than phenomenology of simplified models. Also, there is no obvious explanation in ND theory to the difference between the behaviour in fresh and recovered medium, perhaps because that theory does not even aim to explain the process of propagation block, only development of a dynamic instability.

An interesting theoretical mechanism of finite lifetime of re-entrant waves was suggested long ago by Krinsky [10], within an axiomatic "tau-model", which has some properties that are relevant to cardiac tissue but not captured by FitzHugh-Nagumo type simplified models. Although the mechanism of finite lifetime re-entry of [10] is based on static inhomogeneity of tissue properties and thus not directly applicable to our case, it still can offer some food for thought. A new hope on further progress in understanding the phenomena described in this work comes from recent results on asymptotic properties of realistic models which make them different from traditional simplified models [11, 12].

Acknowledgements. This work was supported in part by grants from EPSRC (GR/S03027/01, GR/S43498/01, GR/S75314/01) and by an RDF grant from Liverpool University.

References

[1] I. V. Biktasheva, V. N. Biktashev, W. N. Dawes, A. V. Holden, R. C. Saumarez, and A. M.Savill. Dissipation of the excitation front as a mechanism of self-terminating arrhythmias. *IJBC*, 13(12):3645–3656, 2003.

[2] J. B. Nolasco and R. W. Dahlen. A graphic method for the study of alternation in cardiac action potentials. *J. Appl. Physiol.*, 25:191–196, 1968.

[3] M. Courtemanche, L. Glass, and J. P. Keener. Instabilities of a propagating pulse in a ring of excitable media. *Phys. Rev. Lett.*, 70:2182–2185, 1993.

[4] A. Karma, H. Levine, and X. Q. Zou. Theory of pulse instabilities in electrophysiological models of excitable tissues. *Physica D*, 73:113–127, 1994.

[5] M. Courtemanche. Complex spiral wave dynamics in a spatially distributed ionic model of cardiac electrical activity. *Chaos*, 6(4):579–600, 1996.

[6] E. M. Cherry and F. H. Fenton. Suppression of alternans and conduction blocks despite steep APD restitution: Electrotonic, memory, and conduction velocity restitution effects. *Am. J. Physiol. - Heart C*, 286:H2332–H2341, 2004.

[7] M. Courtemanche, R. J. Ramirez, and S. Nattel. Ionic mechanisms underlying human atrial action potential properties: insights from a mathematical model. *Am. J. Physiol.*, 275:H301–H321, 1998.

[8] J. Kneller, R. J. Ramirez, D. Chartier, M. Courtemanche, and S. Nattel. Time-dependent transients in an ionically based mathematical model of the canine atrial action potential. *Am. J. Physiol. Heart Circ. Physiol.*, 282:H1437–H1461, 2002.

[9] L. J. Leon, F. A. Roberge, and A. Vinet. Simulation of two-dimensional anisotropic cardiac reentry: effects of the wavelength on the reentry characteristics. *Ann. Biomed. Eng.*, 22:592–609, 1994.

[10] V. I. Krinsky. Fibrillation in excitable media. *Cybernetics problems*, 20:59–80, 1968.

[11] R. Suckley and V. N. Biktashev. Comparison of asymptotics of heart and nerve excitability. *Phys. Rev. E*, 68:011902, 2003.

[12] V. N. Biktashev and R. Suckley. Non-Tikhonov asymptotic properties of cardiac excitability. *Phys. Rev. Letters*, 93:168103, 2004.

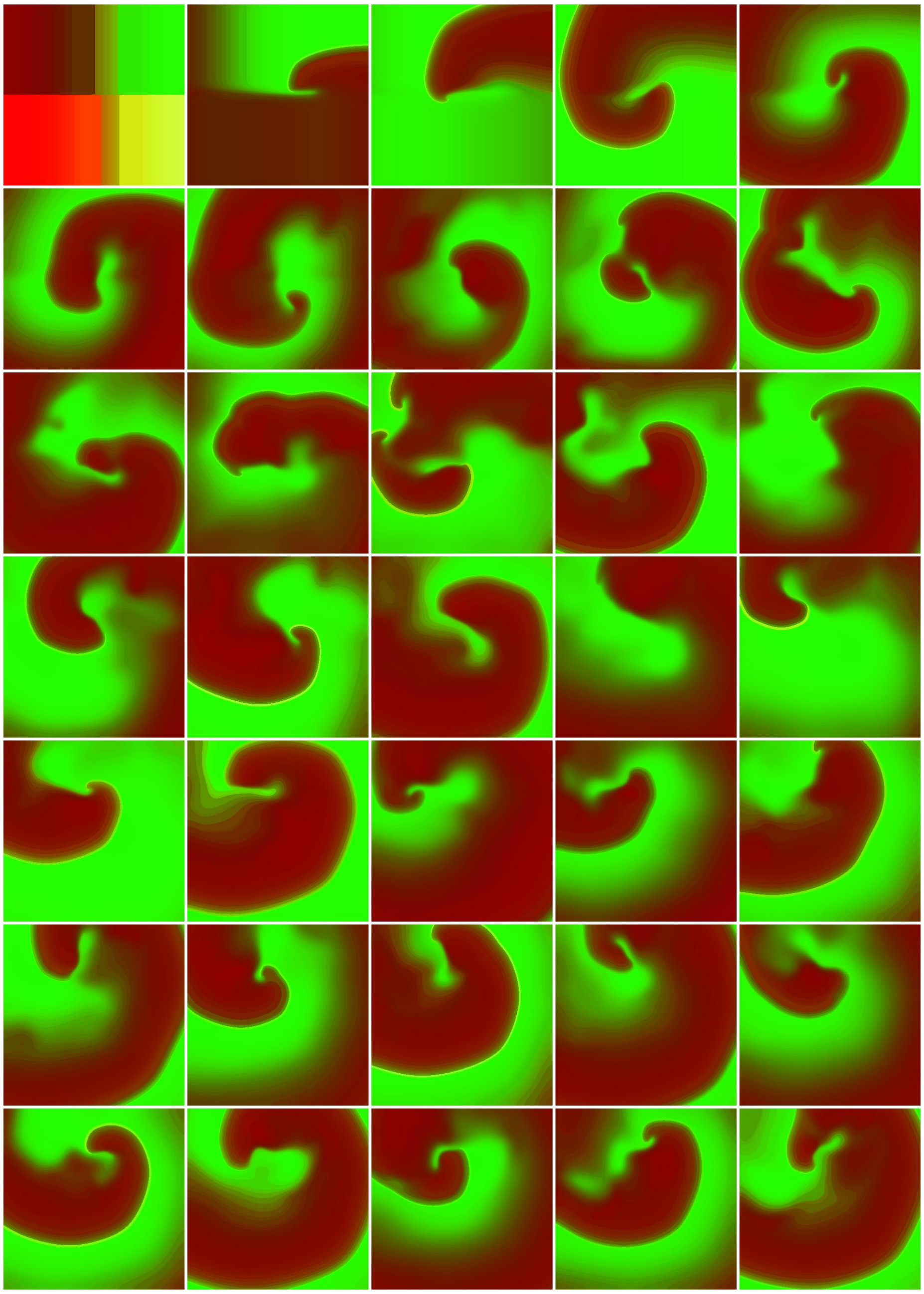

Fig. 4. (color online) Spiral wave in a tired medium. Shown are snapshots with interval 100 ms, starting from 0 ms.

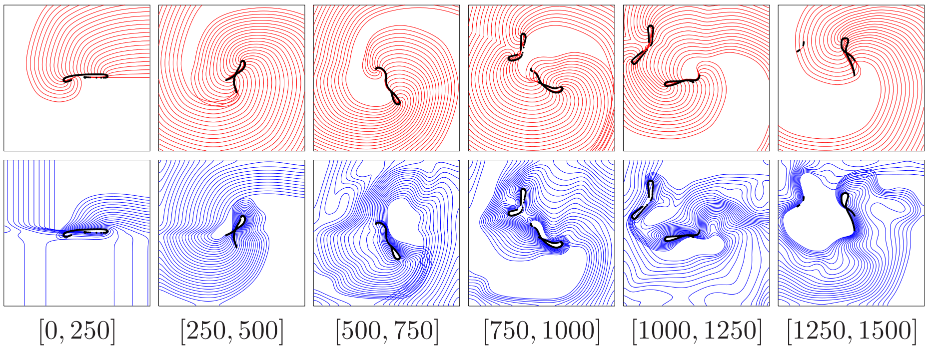

Fig. 5. (color online) Isochronal maps of initial 1800 ms of evolution of a spiral wave initiated by cross-field method in a tired medium. Notations are the same as on fig. 3.

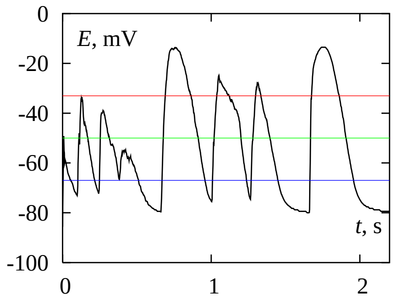

Fig. 6. An electrogram recorded at point with coordinates $(35.2, 35.2)$ mm from the left top corner in the numerics described in figs. 1 and 3. Horizontal lines show the levels at which detection of APD and DI was attempted.

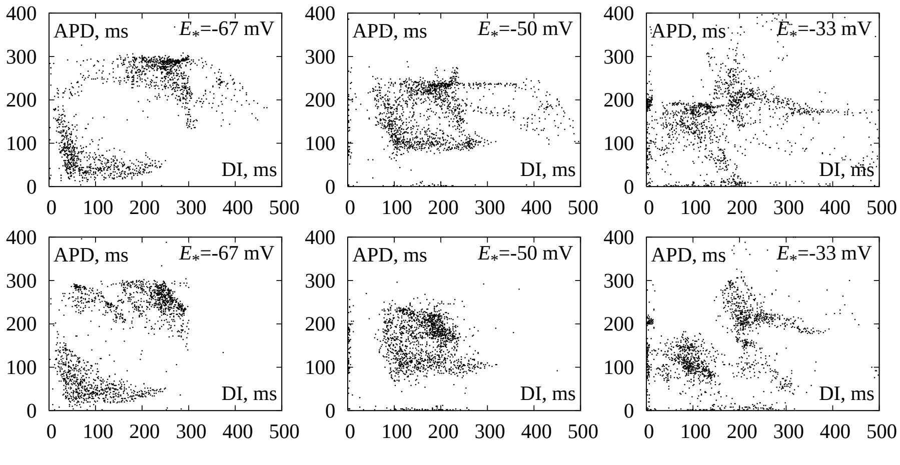

Fig. 7. Graphs of APD vs DI for electrograms at 289 points in the numerics shown on figs. 1 and 3, for different values of E_*. Top row: fresh medium. Bottom row: tired medium.